On the Performance of IEEE 802.11-based Outdoor Networks with Poisson and Self-Similar Traffic

Roger Pierre Fabris Hoefel

***Resumo*—São derivados resultados analíticos que permitem quantificar o desempenho do controle de acesso ao meio empregado nas redes IEEE 802.11. São deduzidas expressões analíticas concernentes ao aumento da interferência externa e da potência transmitida pelos terminais móveis ao implementar-se controle de potência rápido em sistemas DS-CDMA.**

***Palavras-Chave*—Redes locais sem fio, 802.11, CDMA, controle de potência rápido.**

***Abstract*—Analytical expressions are derived in order to assess the IEEE 802.11 medium access control (MAC) protocol performance. Analytical results are derived concerning to the increase of intercellular multiple access interference (MAI) and power transmitted by the mobile stations (MSs) in direct sequence-code division multiple access (DS-CDMA) systems with fast power control (PC).**

***Index Terms*—WLANS, 802.11, CDMA, fast power control.**

I. INTRODUCTION

Wireless local area networks (WLANs) allow several advantages over wired networks (i.e. mobility, easy and speed of deployment, flexibility, operation on unlicensed frequency band, cost, among others). However, WLANs only have become a competitive player in the mass market with the advent of technical solutions that have been efficiently addressed data rate and security issues. These efforts have produced the IEEE 802.11 network technology family tree specifications [1], the High Performance European Radio Local Area Network Type 2 (HIPERLAN/2) standard [2], and Mobile Multimedia Access Communication System. Although these standards are focused on WLANs, recent results have indicated that it is also feasible to deploy outdoor cellular networks based on the IEEE 802.11 protocols [3-4].

This paper is organized as follows. In Section II it is done a brief description of the IEEE 802.11 MAC protocol. In Section III, analytical results are derived in order to investigate the performance of the 802.11 MAC state machine loaded with Poisson traffic. The open literature has focused on the performance analysis of 802.11 networks loaded with Poisson traffic. Therefore, in Section IV, it is carried out a comparative assessment of the MAC 802.11 performance with Poisson and world-wide web (WWW) self-similar traffic. In Section V, analytical expressions are derived to estimate accurately the transmitted power and the uplink intercellular MAI in DS-CDMA systems with fast PC. Finally, conclusions and remarks on future research directions are carried out in Section VI.

Roger Pierre Fabris Hoefel, Department of Telecommunications Engineering, University La Salle (UNILASALLE) , Canoas, Rio Grande do Sul, Brazil, E-mail: roger@lasalle.tche.br.

II. IEEE 802.11 MAC STATE MACHINE

In this paper, it is assumed the High Rate Direct Sequence Spread Spectrum (HR-DSSS) 802.11b specification [1, pp 189], which supports 1, 2, 5.5 and 11 Mbps operating at 2.4 GHz Industrial-Scientific and Medical (ISM) band. The other 802.11 physical layer specifications (e.g. 802.11, 802.11a, 802.11g) use the same 802.11 MAC sublayer, which is mapped to the particular physical layer using a physical layer convergence procedure (PLCP).

The MAC coordination function can operate in the following modes [1, pp. 23], [3]:

1) *Carrier Sense Multiple access with collision avoidance (CSMA/CA)*: It is a contention-based protocol similar to the IEEE 802.3 Ethernet. Physical carrier-sensing and virtual carrier-sensing functions are implemented in order to manage this process. The virtual-carrier sensing is implemented by the Network Allocation Vector (NAV). This timer, which is updated by a control field transmitted in data and control packets, indicates the amount of time the channel will be reserved in order to permit uninterrupted atomic transmissions. This mode is known as distributed coordination function (DCF). It can be used in Infrastructure Base Service Set (IBSS), where access points and wired network backbones are implemented, and Independent BSS (or ad hoc networks) networks;
2) *Priority-based access*: It is a pooling protocol that provides contention-free services for time-bounded traffic in IBSS networks. This model is known in the specification as the point coordination function (PCF).

The two modes are used alternately in time, i.e. a contention-free period propitiated by the PCF is followed by a contention period of the DCF.

As shown in Fig. 1, the IEEE 802.11 uses the following different interframe spacing (IFS) [1, pp. 30], [3]:

1) *Short IFS*: It is the shortest IFS used for highest-priority transmission. The following frames use the SIFS interval: ACK (Acknowledgment) frame; CTS (Clear to Send) frame; the second or subsequent data frames of a fragment burst;
2) *PCF IFS (PIFS)*: It is the interval that the stations

operating under PCF use to gain access to the channel;

3) *DCF IFS (DIFS)*: It is used by the stations to transmit data and management frames in the DCF mode;
4) *Extended IFS (IFS)*: This largest IFS is a waiting period used by the stations when there is an error in frame transmission. This interval provides enough time for the receiving station to send an ACK frame.

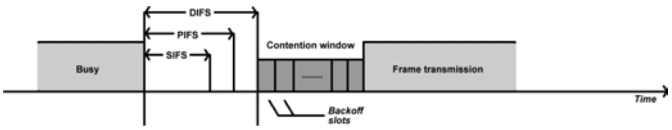

Fig. 1 Interframe spacing relationships.

In this paper, it is assumed that the stations use the DCF in a single cell IBSS network. It is investigated the following access polices [1, pp. 31], [3]:

1) Basic positive acknowledgment (Fig. 2): The terminal only access the channel after implementing the physical carrier-sensing and virtual carrier-sensing functions. If the NAV is zero, then the transmission can begin immediately if the channel has been idle for longer than the DIFS. If the channel is busy, the station must deferral its transmission until the channel becomes idle for a DIFS period. After this DIFS period, the station: *(i)* starts to treat the channel in units of slot time; *(ii)* implements a binary exponential backoff period (EBP) to determine the time slot access time; *(iii)* continues to check the channel to verify if it is busy or idle. If the channel remains idle when the EBP becomes zero, then the terminal starts its packet transmission. Otherwise, the decrement of backoff interval stops and only resumes after the channel be detected idle for the DIFS period. The stations exchange data based on a stop-and-go scheme: the receiver station must transmit an ACK control packet (or piggybacking ACK control information in an unicast data frame) after a SIFS period. If either the data packet or the ACK control packet be corrupted or the timeout expires, then the sender station must use the EIFS to set the time for begin a new physical channel sensing procedure.

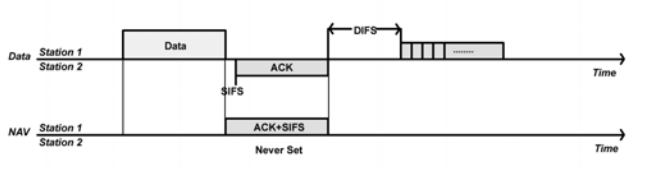

Fig. 2 Atomic basic positive ACK of data.

2) RTS/CTS clearing (Fig. 3): It is used to avoid the hidden terminal problem. This scheme is used to gain the control of the channel for frames larger than the RTS threshold. Initially, the channel is sensed as in the basic positive ACK police. However, the sender station transmits a RTS control frame, instead of a data frame, to reserve the channel. If the transmission is successful, the opposite partner sends a CTS control frame to confirm the reserve. After that, it is transmitted the data unicast frame as in the basic positive ACK scheme. Again, the sender station must use the EIFS to set the time for new physical channel sensing if any data or control are corrupted or due to timeout expiration of the CTS control frame.

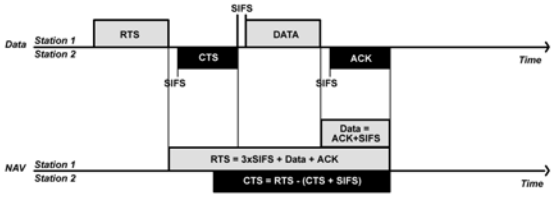

Fig. 3. Atomic RTS/CTS clearing technique.

III. 802.11 DCF THROUGHPUT ANALYSIS FOR POISSON TRAFFIC

A. Analytical results

In this section, it is assumed that the terminals generate Poisson traffic at an infinitesimally small rate resulting in an aggregate channel load of G packets per data packet time L. Therefore, postulating a homogenous propagation time a, the throughput can be stated as:

$$S = \frac{Le^{-aG}}{\overline{T}} = \frac{Le^{-aG}}{\overline{B} + \overline{I}}, \qquad (1)$$

where the numerator models the average amount of time in which a data packet is transmitted without collision. $\overline{T}$ denotes the average cycle time consisting of a busy and an idle period. The average period between packet arrivals is given by $\overline{I} = I/G$.

The expected value of the busy period can be stated as:

$$\overline{B} = P\{succesfull\ \ transmissi\ on\}\overline{B}_{sucs} + P\{unsuccesfu\ ll\ \ transmissi\ on\}\overline{B}_{unsucs}, \qquad (2a)$$

$$\overline{B} = e^{-aG}\,\overline{B}_{sucs} + \left(1 - e^{-aG}\right)\overline{B}_{unsucs}\ . \qquad (2b)$$

Firstly, it is assumed that the atomic data transmission consists of a basic positive ACK of data. Therefore, the average busy time when the transmission is successful is given by (3a) and, correspondingly, given by (3b) when there is a collision.

$$\overline{B}_{sucs} = DIFS + L + a + SIFS + L_{ACK}\ , \qquad (3a)$$

$$\overline{B}_{unsucs} = DIFS + \overline{Y} + L + a\ , \qquad (3b)$$

where L_{ACK} is the transmission time of the ACK control packet.

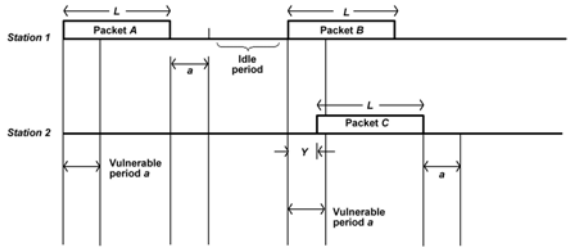

Fig. 4. Busy period with simultaneous transmissions in the vulnerable period a.

According to Fig. 4, the probability density function (PDF) Y is the probability that no arriving packet occurs in an interval of length *(a-y)* given that the packet that originates a collision was transmitted in the time interval y, i.e. [5, pp. 219]:

$$f_Y(y) = G\,e^{-G(a-y)} \quad for\ 0 \le y \le a\ . \qquad (4)$$

Therefore, the average time between the first and the last packet in the busy period is given by:

$$\overline{Y} = a - \frac{1 - e^{-aG}}{G} \cdot \quad (5)$$

On the other hand, if it is used the RTS/CTS clearing technique, then expected duration of successful atomic data transmission is given by:

$$\overline{B}_{sucs} = DIFS + L_{RTS} + a + SIFS + L_{CTS} + a + SIFS + L + a + SIFS + L_{ACK}, \quad (6)$$

where L_{RTS} and L_{CTS} are the transmission times of the RTS and CTS control packets, respectively.

It can be immediately verified that the average time of unsuccessful RTS contention control frame is given by:

$$\overline{B}_{unsucs} = DIFS + \overline{Y} + L_{RTS} + a \, . \quad (7)$$

B. Analytical versus simulation results

In the following results, it is assumed a single-cell IBSS network (such as it is only used the DCF MAC protocol to transmit the non-real time traffic) and an ideal channel (the only source of packets errors are the possible collisions in the contention window, CW). The assumed default parameters are: slot time of 20 μs, SIFS of 20 μs and DIFS of 50 μs. The fragmentation threshold is set to 2308 bytes (i.e. the maximum payload length when the Wired Equivalent Protocol, WEP, is operational).

For an IBSS 802.11 network, the MAC header consists of 28 bytes [1, pp. 58] plus 4 bytes for the WEP [1, pp. 91]. Assuming a data rate of 1 Mbps, then the transmission time for an Ethernet 1500 bytes packet is of L=12.25 ms and L=4.86 ms for a 576 typical Web browsing datagram. Correspondingly, the transmission times for RTS (160 bits), CTS (112 bits) and ACK (112 bits) control frames are, respectively, given by 160μs, 112μs and 112μs [1, pp. 60].

Fig. 5 shows an excellent agreement between analytical and simulation results for propagation times of *2μs* and *L/2*. While the former propagation time models a realistic scenario (i.e. WLAN of 600m), the last one is only included to validate the simulator in environments where the propagation time *L* is a significant fraction of the packet transmission time. Naturally, with *a=L/2* the timers of MAC Management Information Base (MIB) were set up to support an uninterrupted atomic data operation in this hypothetical environment (i.e. even with *a=L/2* the virtual channel sensing avoids the collision between the ACK control packet and the next data packet and it is also assumed that the packets are not dropped due to excessive delay). It is also observed that the RTS/CTS clearing does not impact the throughput in as much as the packet transmission time *L* is significantly greater than the transmission time of the clearing control packets. Due to the assumed aggregated Poisson traffic assumption, the CW resolution of the 802.11 MAC protocol was not implemented in this case (i.e. the packets are dropped after the first non-successful transmission attempted), and, therefore, the simulated aggregated traffic follows strictly the Poisson statistics. Finally, it is pointed out that the shown results indicate the correctness of the IEEE MAC 802.11-based simulator that has been developed in C^{++} using object oriented paradigm approach.

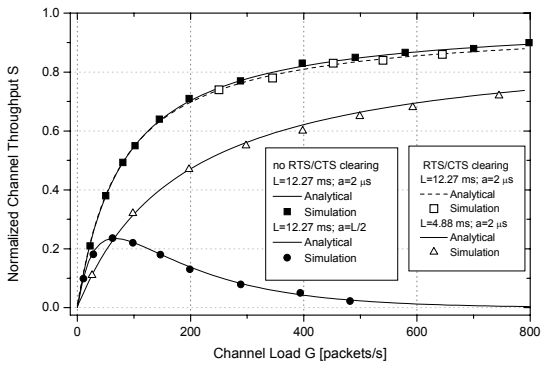

Fig. 5. Comparison between simulation and analytical results.

IV. SIMULATION RESULTS FOR WEB BROWSING

In this section, it is used simulation to assess the performance of a 802.11 network loaded with self-similar traffic.

Firstly, it is described the traffic models used:

1) *European Telecommunication Standardization Institute (ETSI) Web browsing traffic mode* [6, pp. 247]: In a data section, a MS performs one or more packet call requests, which is a geometric random variable (RV), N_{pc}, with mean μ_{Npc} of 5. The interarrival time between two packet call requests, D_{pc}, is an exponential RV with mean μ_{Dpc} of 4 s. A new packet request only starts when the opposite partner receives all packets of the earlier call request. The number of packets in a packet call request, N_d, is geometrically distributed with mean μ_{Nd} of 25. The interarrival packet time inside a packet call is an exponential RV with mean μ_{Dpc} of 64.12 ms. The size of packets in bytes is modeled by a truncated Pareto distribution with a shape parameter (or Noah parameter) of 1.1, a location parameter of 81.5 and a maximum value of 67 kbytes. This model produces an average IP datagram of 481 bytes and, consequently, an average rate of approximately 64 kbps (481*8/0.5). In [6], the average rate is 8 kbps as much as μ_{Dpc}=0.5 s. In this paper, it is not considered that the packets storaged in the first-in first-out queue can be dropped due to the overflow.
2) *Email traffic* [6, pp. 250]: It is assumed that a single email message is generated per session. The message length follows a truncated Pareto distribution with Noah parameter of 1.01 and a location parameter of 1.4 kbytes. The minimum and maximum message size are given by 1.4 kbytes and 500 kbytes, respectively. This model produces an average IP datagram of 9423 bytes.
3) *Poisson traffic*: It is generated assuming an interarrival time of 64.12 ms and a deterministic payload length of 481 bytes, totalizing an input rate of 64 kbps, 8.0*(481+32) bits/64.12 ms, per terminal.

Hereafter, the 802.11 CW scheme is operational such as the backoff time is a RV uniformly distributed between 0 and CW_{max}-1 time slots, where CW_{max} is set using a binary exponential algorithm [1, pp. 34]. It is assumed a data rate of 5.5 Mbps. However, the MAC header and control packets are transmitted at 1 Mbps. Unlimited retransmissions are done, i.e. the long retry counter was set to an enough high value that avoids the packets be dropped due to an excessive number of collisions in the CW.

As it is assumed that RTS/CTS clearing is used in all

transmission, then the maximum value of the throughput for a Poisson traffic without fragmentation is given by $S_{max}=0.656$ for $a=2$ μs. Fig. 6 shows that the maximum throughput obtained for Poisson input traffic is very close to this asymptotic value. It is also noticed a reasonable agreement between numerical and simulation results for Poisson traffic and $a=25$ μs. The theoretical values were calculated, as required by $\bar{I}$ I in (1), using the non-normalized values of G.

Fig. 6 also shows that the maximum efficiency is greater for WWW browsing due to the reducing of RTS/CTS overhead as such there is a high probability that packets above the assumed fragmentation threshold (i.e. 2308 octets) are generated due to self-similarity of Pareto distribution. However, Fig. 7 shows that the transmission delay observed with self-similar web traffic is substantially greater in relation to that one observed with Poisson traffic. The delay statistics for email traffic have shown that larger delays can be expected due to the attachments of data files.

It is observed that the processing time at the nodes was neglected in Figs. 6 and 7. Therefore, supposing that the time out for the ACK control packet is equal to the DIFS [3], then the maximum one-way propagation delay is equal to 25μs (i.e. a cell size of 7.5 Km). Neglecting the hidden node problem and noticing that the terminals physically sensing the channel by the DIFS period, the DIFS (i.e. 50 μs) will be the upper bound for the one-way propagation delay in order to avoid the collision of ACK control packets with the beginning of the next atomic period. Comparing the results for $a=50$ μs and $a=100\mu s$, Fig. 6 has shown that the collision of ACK packets do not affect substantially the throughput for the range of channel load investigated. Obviously, the buffer time out must be adjusted to avoid packets being dropped due to excessive delay.

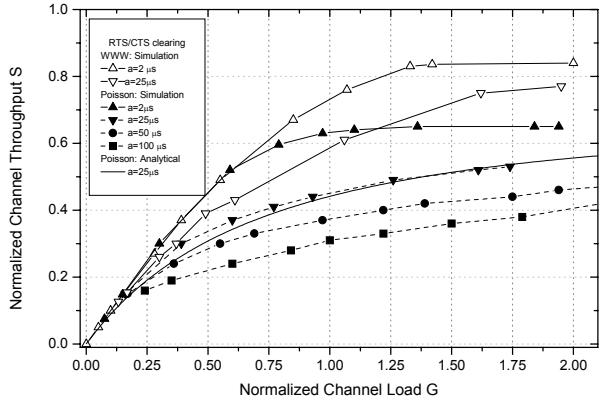

Fig. 6. Throughput as a function of the normalized channel load, propagation delay and kind of traffic.

V. ANALYTICAL RESULTS FOR FAST POWER CONTROL IN THE UPLINK OF DS CDMA SYSTEMS

It is assumed a coherent binary phase-shift keying (BPSK) DS-CDMA interference limited system where a slow PC scheme compensates perfectly the long and medium-term fading due to the log-linear propagation model with path loss exponent Γ, and a lognormal shadowing with standard deviation σ_{dB}. Therefore, if the multiple access interference (MAI) is modeled as a flat power spectrum density, then the

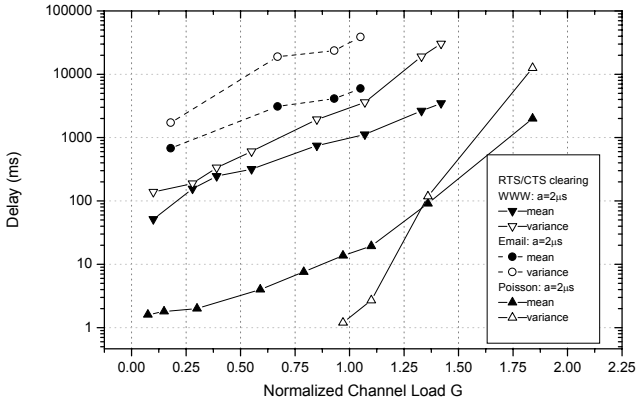

Fig. 7. Statistics of delay for WWW, Email and Poisson traffic for a propagation time of 2 μs.

uplink signal-to-interference-ratio (SIR) for the *k-th* mobile station (MS) at the output of a maximum ratio combiner (MRC) receiver with M spatially uncorrelated antennas and P fingers per antenna can be stated as:

$$SIR_k = \beta_k G_p \sum_{n=1}^{M} \frac{\sum_{l=1}^{P} \alpha_{k,n,l}^2}{E\left[\sum_{\substack{j=1 \\ j\neq k}}^{K} \beta_j \sum_{l=1}^{L} \alpha_{j,n,l}^2\right] + KE[\beta] f} = G_p \beta_k \frac{S_k}{I}, \tag{8}$$

where G_p is the processing gain and K is the number of active MSs in each cell. The positive real number f models the average relative other-cell interference factor when only the slow PC is operational [7, pp. 314]. The short-term channel gain for the *k-th* MS at the *l-th* finger in the *n-th* antenna is modeled as an $\alpha_{k,n,l}$ Nakagami-m RV, whose PDF is given by:

$$p(\alpha_{k,n,l}) = M(\alpha_{k,n,l}, m, \Omega_l) = \frac{2}{\Gamma(m)} \left(\frac{m}{\Omega_l}\right)^m \alpha_{k,n,l}^{2m-1} exp\left(-\frac{m}{\Omega_l}\alpha_{k,n,l}^2\right) \quad for\ \alpha_{k,n,l} > 0, \tag{9}$$

where $\Gamma(.)$ is the gamma function, $1/m$ ($m\geq 0.5$) is the fading figure and Ω_l is the second moment of the RV α [2] The subscripts k and n in Ω_l were dropped since it is postulated that the same average power is received in each antenna for every MS. An exponential negative (EN) multipath intensity profile (MIP) can be modeled as:

$$\Omega_l = \Omega_0 exp(-\delta l) \quad for \quad \delta \geq 0;\ l = 1,...,L, \tag{10}$$

where L is the number of resolvable multipaths ($L\geq P$). Ω_0 takes into account the normalization of channel gain per antenna, i.e.

$$\sum_{l=1}^{L} E\left[\alpha_{k,n,l}^2\right] = \sum_{l=1}^{L} \Omega_l = 1 \quad for\ n = 1;\cdots, M, \tag{11}$$

and δ controls the decaying of the average path strength as a function of the path delay. The EN MIP reduces to an equal strength (ES) MIP if $\Omega_0=1/L$ and $\delta=0$.

A. Fast power control scheme

It is assumed a fast PC scheme where the received signal power at the MRC receiver output is set in a pre-established

value. Hence, ideally this fast PC scheme sets the power transmitted by the *k-th* MS at:

$$\beta_k = \frac{M}{\sum_{n=1}^{M}\sum_{l=1}^{P}\alpha_{k,n,l}^2} = \frac{M}{S_k}. \quad (12)$$

Without the fast PC scheme, the average signal power at the BS MRC receiver output is given by (see 8 and 11):

$$\overline{S} = E\left[\sum_{n=l=1}^{M}\sum^{P}\alpha_{k,n,l}^2\right] = \frac{MP}{L}, \quad (13)$$

Otherwise, using (12) in (8), the average received signal power with fast PC at the MRC receiver output is given by:

$$\overline{S} = \beta_k \sum_{n=1}^{M}\sum_{p=1}^{P}\alpha_{k,n,p}^2 = M \quad (14)$$

Therefore, if there is a mismatch between MRC and channel inbound diversity, then the average received power is only decreased in systems without fast PC.

B. Fast power control statistics

The sum of squares of independent $M(x_i, m, \Omega_i)$ RVs, i.e.

$$y = \sum_{i=1}^{P} x_i^2, \quad (15)$$

may be approximated as a Gamma RV [8]:

$$p(y) = Gamma\ (y, m_s, \Omega_s) = \frac{1}{\Gamma(m_s)}\left(\frac{m_s}{\Omega_s}\right)^{m_s} y^{m_s-1} exp\left(-\frac{m_s}{\Omega_s}y\right) \quad for\ y>0, \quad (16)$$

$$m_s = \frac{\left(\sum_{i=1}^{P}\Omega_i\right)^2}{\sum_{i=1}^{P}\frac{\Omega_i^2}{m}}, \qquad \Omega_s = \sum_{l=1}^{P}\Omega_i. \quad (17)$$

where m_s and Ω_s/m_s are, respectively, the shape and scale parameters.

It is noticed that if every x_i in (15) is $M(x_i, m, \Omega)$ distributed (i.e. $\Omega_i=\Omega$ for i=1,…P), then (15) is *Gamma(y, Pm, PΩ)* distributed.

It can be demonstrated that the PDF of RV $z=1/y$ is given by:

$$p(z, m_s, \Omega_s) = \frac{1}{\Gamma(m_s)}\left(\frac{m_s}{\Omega_s}\right)^{m_s} z^{-(m_s+1)} exp\left(-\frac{m_s}{\Omega_s}\frac{1}{z}\right) \quad for\ z>0. \quad (18)$$

with shape and scale parameters given by m_s and m_s/Ω_s, respectively. The mean and variance of the RV z exist for certain values of the shape parameter, i.e.

$$E[z] = \frac{m_s/\Omega_s}{(m_s-1)} \quad for\ \ m_s > 1, \quad (19)$$

$$var[z] = \frac{(m_s/\Omega_s)^2}{(m_s-1)^2(m_s-2)} \quad for\ m_s > 2. \quad (20)$$

Hereafter, an RV that follows (18) will labeled as reciprocal Gamma distributed, i.e. *RGamma(z, m_s, Ω_s)*.

Based on the procedure above outlined, it can be checked that the transmitted power is $RGamma(\beta, MPm, P/L)$ distributed for an ES MIP Nakagami-m fading channel.

Finally, using (10) in (17) it can be also verified that the transmitted power with fast PC is *RGamma(β, Mm_s, Ω_s)* distributed for an EN MIP Nakagami-m fading channel.

C. Analytical versus simulation results

Unless otherwise cited, it is assumed the following: *(i)* a Nakahmi-m fading with *m=1* (i.e. a Rayleigh fading channel); *(ii)* a fast PC scheme that sets the power at the MRC output in a pre-established value; *(iii)* a macrocellular hexagonal network with 37 BSs, *Γ=4* and σ_{dB}*=8 dB*; *(iv)* that the MSs selects the BS to which the minimum average transmission power is required. Using the analytical results derived in [7, pp. 311], then it can be verified that the normalized mean, *f*, and the normalized standard deviation, σ_f, of the external MAI are given by *0.6* and *0.44* respectively, when only the slow PC scheme is operational.

Fig. 8 is a minor sample of extensive investigations that indicate an excellent agreement between numerical and simulation results (i.e. the transmitted power with fast PC is distributed according 18). It can be found analytical results for the average transmitted power due to the fast PC scheme [9]. However, Fig. 8 shows that the standard deviation of the transmitted power statistics also must be taken into account in environments where the requirements for fast PC are more demanding, i.e. when the effective diversity at the receiver is not great enough to counterbalance the fast fading.

Fig. 9 shows that the spatial diversity can be used to reduce substantially the transmitted power due to the fast PC scheme. It is also noticed that the increase of the power in the LOS path, represented by the increase of parameter *m*, reduces the transmitted power.

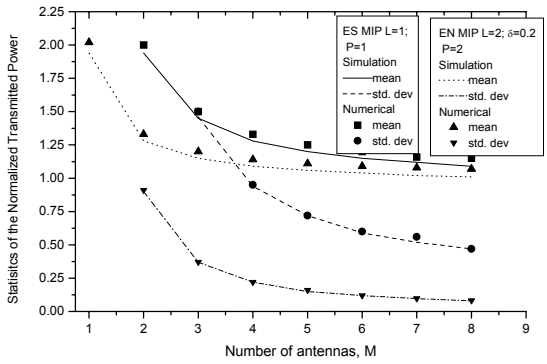

Fig. 8. Numerical and simulation results for the mean and standard deviation of the transmitted power due to the fast PC.

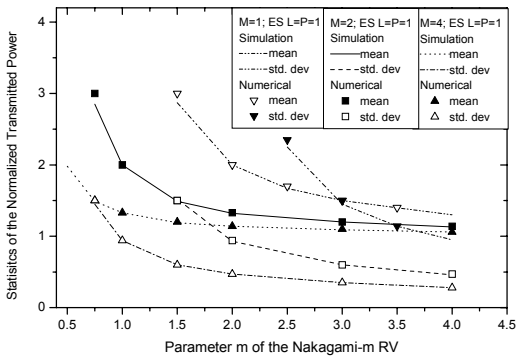

Fig. 9. Numerical and simulation results for transmitted power statistics due to the fast PC.

Fig. 10 shows again an excellent agreement between numerical and simulation results, except in environments where there is no spatial diversity. This occurs due to (17) does not provide an adequate fitting in environments with low effective diversity and large difference between the average power of the two paths. These figure also show that the increase of the spatial and inbound diversity leads to a reduction of the transmitted power due to the fast PC .

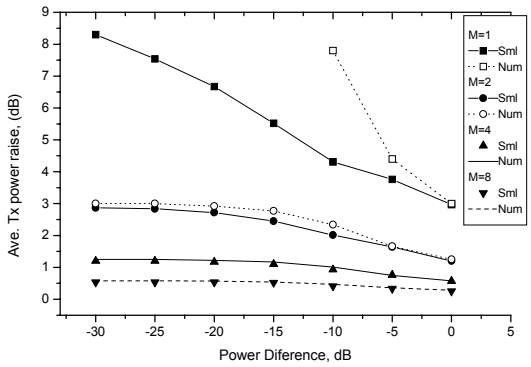

Fig. 10. Numerical and simulation results for the average transmitted power raise due to the fast PC scheme as a function of average power difference of the two paths. P=L=2.

The fast PC increases the other-cell interference factor estimated when uniquely a slow PC is operational. As it shown at item B of this Section, the transmitted power is *RGamma(*β, Mm_s, Ω_s*)* distributed when it is used the fast PC scheme, and, therefore, the normalized average and variance of the other-cell interference factor with fast PC can be estimated by:

$$f_{fpc} = \frac{Mm_s/\Omega_s}{(Mm_s - 1)} f \quad for \;\; Mm_s > 1, \tag{21}$$

$$\sigma^2_{fpc} = \frac{(Mm_s/\Omega_s)^2}{(Mm_s - 1)(Mm_s - 2)}\left(\sigma^2_f + f^2\right) - f^2_{fpc} \quad for \;\; Mm_s > 2, \tag{22}$$

Using the causal form of the central-limit theorem [10, pp.234], it is possible to model the external interference by a gamma (or chi-squared) RV, whose mean and variance are obtained by multiplying the normalized values of mean and variance by the mean number of users loading the channel.

Fig. 11 shows a comparison between simulated and numerical values of the intercellular MAI cumulative distribution function (CDF) when the ES MIP Rayleigh fading channel is uniformly loaded with 10 MS in all cells. Besides to show an excellent agreement between numerical and simulation results, these results also indicate a meaningful increase in the intercellular MAI when the fast PC scheme is applied on a Rayleigh channel with insufficiently diversity (i.e. L=P=2). It is remarked that de intercellular MAI is not dependent upon the channel inbound diversity when it is implemented an ideal slow PC scheme that only aims at compensating the path loss and the lognormal shadowing.

VI. FINAL REMARKS

As far as it has been presented several results that validate a C^{++} object oriented simulator that implements some essential

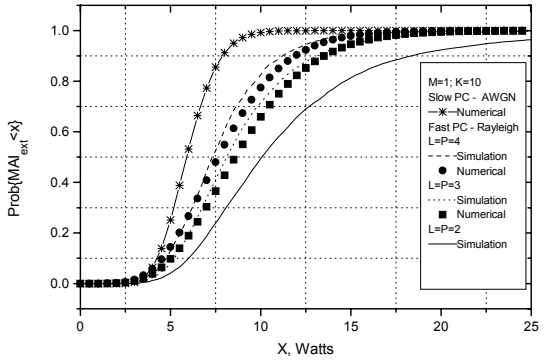

Fig. 11. Comparison between simulated and numerical results of the external MAI CDF when a ES MIP Rayleigh fading channel is uniformly loaded with 10 MS in all cells.

features of the IEEE 802-11 MAC state machine.

Expressions have also been derived in order to estimate the increase of transmitted power and intercellular MAI due the uplink fast PC on DS-CDMA systems. These results can be used to obtain analytical insights on the interrelations between the spatial domain characteristics, transmit power increase and intercellular MAI increase when it is implemented fast PC in the IEEE 802.11-based outdoor networks.

In the future, it is scheduled to take into account the effects of intercellular MAI and multipath fading on the performance of joint operation of DCF and point coordination protocols in 802.11b based ESS network loaded with self-similar traffic and with a modified protocol stack in order to contemplate bi-dimensional (2D) Rake receivers, fast PC, link level adaptation techniques and scheduling schemes [11-12].

REFERENCES

[1] M. S. Gast, *802.11 Wireless Networks*. O'Reilly, 2002.

[2] J. Heiskala and J. Terry, *OFDM Wireless LANs: A Theoretical and Practical Guide.* Sams Publishing, 2001.

[3] K. K. Leung, B. MacNair, L. J. Cimini Jr. and J. H. Winters, "Outdoor IEEE 802.11 Cellular Networks: MAC Protocol Design and Performance," *Proc. of IEEE International Conference on Communication*, v. 1, pp. 595-599, 2002.

[4] M. V. Clark, K. K. Leung, B. McNair and Z. Kostic, "Outdoor IEEE 802.11 Cellular Networks: Radio Link Performance," *Proc. of IEEE International Conference on Communication*, 2002.

[5] G. E. Kaiser, *Local Area Networks. Mc-Graw-Hill, 1988*

[6] A. Brand, H. Aghvami, *Multiple Access Protocols for Mobile Communications.* John Wiley and Sons, 2002.

[7] R. Steele, C-C. Lee and P. Gould, *GSM, cdmaOne and 3G Systems.* John Wiley & Sons, 2001.

[8] T. Eng and L. B. Milstein, "Coherent DS-CDMA Performance in Nakagami Multipath Fading," *IEEE Trans. on Communications*, vol. 43, no. 2/3/4, pp. 1134-1143, Feb/Mar/April 1995.

[9] K. Sipilä, J. Steffens, A. Wacher and M. Jäsberg, "Modeling the Impact of the Fast Power Control on the WCMA Uplink," *Proc. of IEEE 54th Vehicular Technology Conference*, TX, USA, Spring 1999.

[10] A. Papoulis, *Fourier Integral and Its Applications.* McGraw-Hill, 1962.

[11] R. P. F. Hoefel and C. de Almeida, "Effects of Dynamic Time Slot Scheduling Schemes and Soft Handoff on the Performance of TDD DS CDMA Systems with 2D Rake Receivers over a Nakagami-m Frequency Selective Fading Channel", *to be appear in the Special Issue of Journal of the Brazilian Telecommunications Society*, June 2003.

[12] R. P. F. Hoefel, "Dynamic time slot scheduling schemes for an uplink polling MAC TDD DS-CDMA protocol with adaptive antennas," *Electronic Letters*, vol. 38, no. 19, pp. 1131-1133, 2002.